Supplementary Materials for

Transdermal Cold Atmospheric Plasma-Mediated Immune Checkpoint Blockade Therapy

Guojun Chen[a,b,c,1], Zhitong Chen[d,1], Di Wen[a,b,c], Zejun Wang[a,b,c], Hongjun Li[a,b,c], Yi Zeng[a,b,c], Gianpietro Dotti[e], Richard E. Wirz[d,2], and Zhen Gu[a,b,c,f,2]

Correspondence to: guzhen@ucla.edu (Z.G.); wirz@ucla.edu (R.E.W.)

This PDF file includes:

Supplementary text

Figs. S1 to S19

Legend for Movie S1

SI Reference

Other Supplementary Materials for this manuscript include the following:

Movie S1 (.mp4)

www.pnas.org/cgi/doi/10.1073/pnas.1917891117

Materials and Methods

Materials, cell lines, and animals

Polyvinylpyrrolidone and polyvinyl alcohol were purchased from Sigma-Aldrich. Anti-PDL1 antibody (aPDL1) was obtained from Biolegend Inc. The murine B16F10 melanoma cell line was purchased from UNC tissue culture facility. The B16F10-fLuc cell line was purchased from Imanis Life Sciences. Cells were cultured in DMEM (Invitrogen) with 10% FBS (Invitrogen) and 100 U/mL penicillin/streptomycin (Invitrogen) at 37 °C in 5% CO_2. Female C57BL/6 mice (4-5 weeks) were purchased from Jackson Lab. All mouse studies were carried out following the protocols approved by the Institutional Animal Care and Use Committee at the University of California, Los Angeles (UCLA).

CAP device configuration

The CAP device (Fig. S1) was developed by employing a 3D printer (LulzBot TAZ 6) at UCLA. It consists of a two-electrode assembly with a powered needle electrode and a grounded outer ring electrode, which were connected to a high voltage transformer. Operating conditions are discussed in the main text.

Optical emission spectroscopy

A fiber-coupled optical spectrometer (LR1-ASEQ Instruments) was employed to detect CAP generated ROS and RNS (such as nitric oxide [NO], nitrogen cation [N_2^+], atomic oxygen [O], and hydroxyl radicals [•OH]). The optical probe was placed at a radial distance of 10 mm from the center of the CAP jet. Data were collected with an integration time of 10000 ms.

Preparation of aPDL1-loaded hMN patch

All MN patches were prepared using silicone molds with arrays of conical holes machined by laser ablation (Blueacre Technology Ltd.). Each MN had a 300 μm by 300 μm round base tapering to a height of 700 μm. MNs

were arranged in a 15 × 15 array with a 600 μm center-to-center spacing. DI water was directly deposited by pipetting onto each silicone micromold surface, followed by vacuum for 5 min to allow the solution to flow into the cavities. Thereafter, 0.2 mL of 10% PVP/PVA solution (1/1 weight ratio) containing 200 ng of aPDL1 was directly deposited by pipetting onto the silicone micromold surface. After desiccation was completed, needle arrays were carefully separated from the silicone molds and were stored at a desiccator under vacuum. For the preparation of sMN patches, 1.0 mL of 10% PVP/PVA solution (1/1 weight ratio) was deposited onto the silicone micromold instead.

Mechanical strength test

Mechanical strength of microneedles with a stress-strain gauge was determined by pressing a stainless steel plate against MNs on an Instron tensile testing machine. The initial gauge was 2.0 mm between the tips of MN and the plate, with 10.0 N as the load cell capacity. Speed of the plate approaching MNs was set as 0.1 mm/s.

aPDL1 release profile

The amount of aPDL1 released from MNs was detected by ELISA (IgG ELISA Kit, Thermofisher) according to the manufacturer's protocol. The release of aPDL1 from the MN patch was tested in buffer solutions (2 mL, pH=7.4 or 6.5) in a glass container at 37°C under mild shaking (50 rpm/min). A MN patch was attached to a piece of aluminum foil allowing it floating on the aqueous solutions. At pre-determined time points, 100 μL of the medium was collected for analysis and an additional 100 μL of the fresh medium was added.

aPDL1 binding affinity test

The bioactivity of aPDL1 release from MN patches was evaluated using an ELISA assay. Corning Costar 9018 ELISA plate was coated with purified mouse PDL1 protein (Abcam, cat no. ab130039). The plate was sealed and incubated overnight at 4 °C. After washing and blocking, the samples of aPDL1 were added into wells at

room temperature for 2 hours. After washing, HRP-conjugated anti-rat lg(H+L) mAbs (Invitrogen, cat no. 62-9520) were added into wells at room temperature for 1 hour followed with washing. TMB substrate solution was added for the detection of the aPDL1 binding affinity. Free aPDL1 was used as a control.

In vitro DC maturation

Dendritic cells (DCs) were isolated from the bone marrow according to an established method (1). DC maturation was tested in a transwell culturing system, where the upper and lower chambers cultured with B16F10 cancer cells and DCs, respectively. B16F10 cells were treated with CAP and were then co-cultured with DCs for 24 h. DCs were then collected and stained with $CD80^+$ and $CD86^+$ maturation marker-specific antibodies and were subsequently analyzed by a flow cytometer (LSRII (IMED), Beckman).

In vivo tumor models and treatment

1×10^6 B16F10-fLuc cells were transplanted into the right flanks of mice. Six days later, mice were divided into six groups (n=7). Tumor-bearing mice were treated one time with either CAP, solid MN/CAP (sMN/CAP), hMN/CAP (hMN/CAP), aPDL1-loaded hMN (hMN-aPDL1), or aPDL1-loaded hMN/CAP (hMN-aPDL1/CAP). Mice without any treatment served as control. For CAP treatment, mice were anesthetized and a CAP jet was applied on the center and 2 cm above the tumor sites/MN for 4 min. Temperature changes were monitored by FLIR® thermal camera. The tumor volume was measured by a digital caliper and was calculated according to the following formula: $\text{width}^2 \times \text{length} \times 0.5$. The tumor growth also was monitored by an *in vivo* imaging instruments (IVIS) Spectrum System (Perkin Elmer Ltd). For the distant tumor model, 1×10^6 B16F10-fLuc cells were inoculated into both left and right flanks of mice. Tumors in the right flank were treated with hMN-aPDL1/CAP as described above. Animals were euthanized when showing signs of imperfect health or when the size of tumors exceeded 1.5 cm^3.

Flow cytometry

Tumors and draining lymph nodes were collected 3 days after different treatments, cut into small pieces, and homogenized to form a single cell suspension. Cells were stained with fluorescence-labeled antibodies. The stained cells were measured on an LSRII (IMED) flow cytometer (BD Biosciences) and analyzed by the FlowJo software package (version 10.0.7; TreeStar, USA, 2014). For DC maturation tests: CD80 (Biolegend, cat no. 104707, PE-labeled), CD86 (Biolegend, cat no. 105011, APC-labeled), and CD11c (Biolegend, cat no. 117343, Brilliant Violet 421-labeled). For ICD analyses: calreticulin (Abcam, cat no. ab196159, Alexa Fluor® 647-labeled). For T cell analyses: CD3 (Biolegend, cat no. 100228, Brilliant Violet 421-labeled), CD4 (Biolegend, cat no. 100408, PE-labeled; cat no. 100422, PE/Cy7-labeled), CD8 (Biolegend, cat no. 100712, APC-labeled), CD25 (Biolegend, cat no. 102012, APC-labeled), FoxP3 (Biolegend, cat no. 126404, PE-labeled), Ki67 (Biolegend, cat no. 652410, FITC-labeled), and Granzyme B (Biolegend, cat no. 396404, FITC-labeled). Compensation was performed for T cell analyses. All antibodies were used following the manufacturers' instructions. Antibodies were diluted 500 times except for CD3 (100 times).

Immunofluorescence staining

Tumors were harvested from the mice in different groups and frozen in the optimal cutting temperature (OCT) medium. Tumors were cut *via* a cryotome, mounted on slides, and stained with Alexa Fluor® 594 anti-mouse CD8a antibody (Biolegend, cat no. 100758) and Alexa Fluor® 488 anti-mouse CD4 antibody (Biolegend, cat no. 100425) overnight at 4 °C. The concentration of these antibodies used in the experiments was 20 μg/mL. Cell nuclei were stained with Hoechst 33342 (Thermo-Fisher Scientific). The slides were recorded using a confocal microscope (Leica TCS-SP8 Confocal Microscope). Hoechst 33342 was excited with a 405 nm laser; Alexa Fluor® 488 was excited with a 488 nm laser; and Alexa Fluor® 594 was excited with a 561 nm laser. The imaging channels were set at 450-500 nm, 500-550 nm, and 570-620 nm, respectively.

Cytokine detection

The serum levels of IL-2 (Biolegend, cat. no. 431001), IL-12p70 (Biolegend, cat. no. 433607), IL-6 (Biolegend, cat. no. 431304), IFN-γ (Biolegend, cat. no. 430801), and TNF-α (Biolegend, cat. no. 430904) were measured with ELISA kits according to the manufacturer's instructions. Serum samples were isolated from mice 3 days after treatment.

Statistical analysis

All results are presented as means ± standard error of the mean (SEM). Tukey post-hoc tests and one-way ANOVA were used for multiple comparisons (when more than two groups were compared), and Student's *t*-test was used for two-group comparisons. Survival benefit was determined using a logrank test. All statistical analyses were carried out with Prism software package (PRISM 7.0; GraphPad Software). The threshold for statistical significance was $P<0.05$.

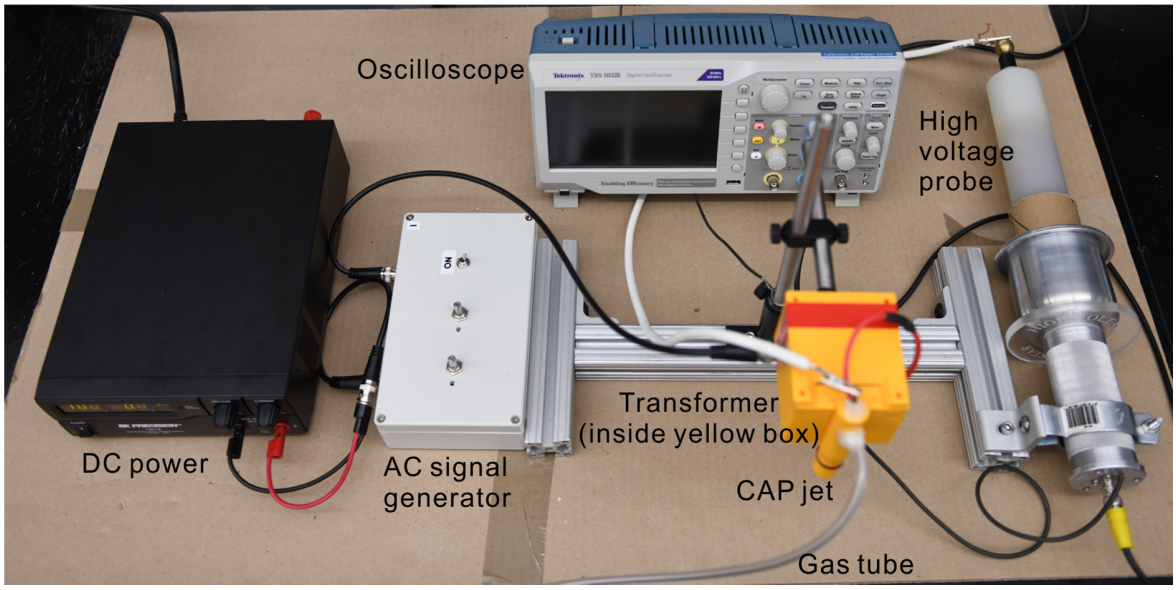

Fig. S1. CAP set-up configuration, including DC power, AC signal generator, high voltage probe, oscilloscope, transformer, a CAP jet assembly, and a gas feed tube.

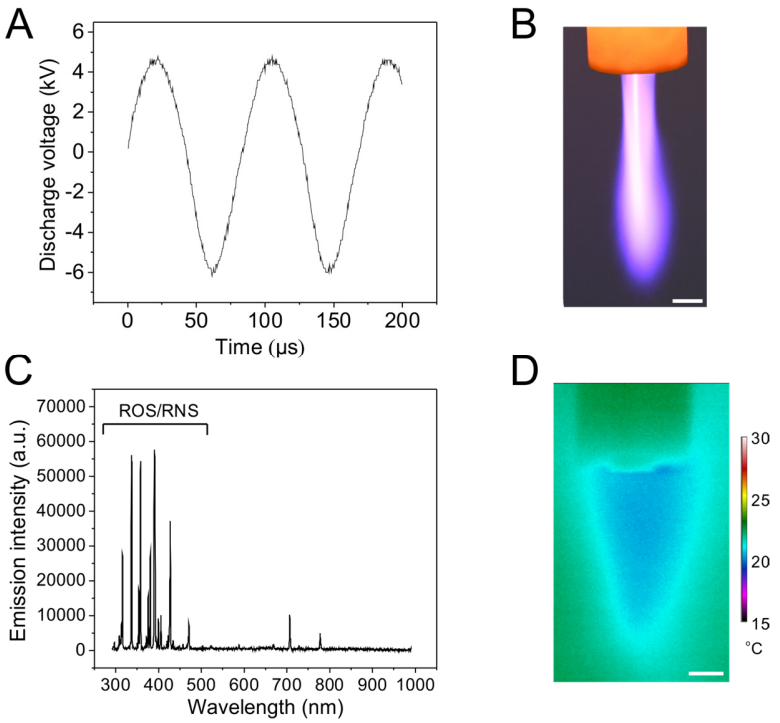

Fig. S2. Characterization of the CAP setup. (**A**) Typical discharge voltage, frequency, and waveform for the CAP device. (**B**) Photograph of the generated CAP jet. Scale bar, 0.5 mm. (**C**) A typical OES spectrum of CAP. (**D**) Temperature measurement of the generated CAP. Scale bar, 0.5 mm.

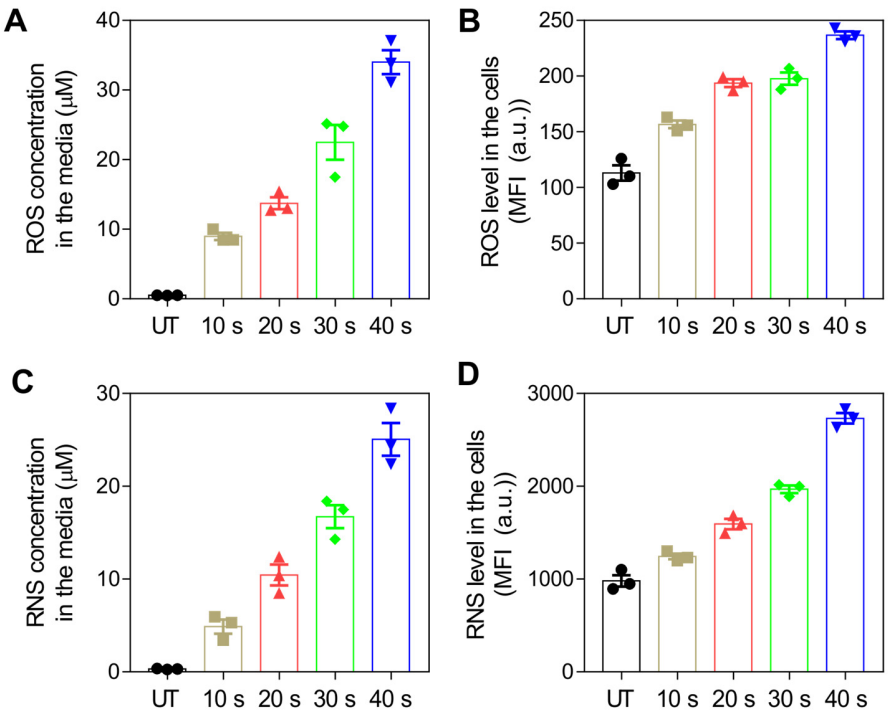

Fig. S3. ROS concentration in the (**A**) media and (**B**) cells after CAP treatment (*n*=3). RNS concentration in the (**C**) media and (**D**) cells after CAP treatment (*n*=3). Data are presented as mean ± SEM.

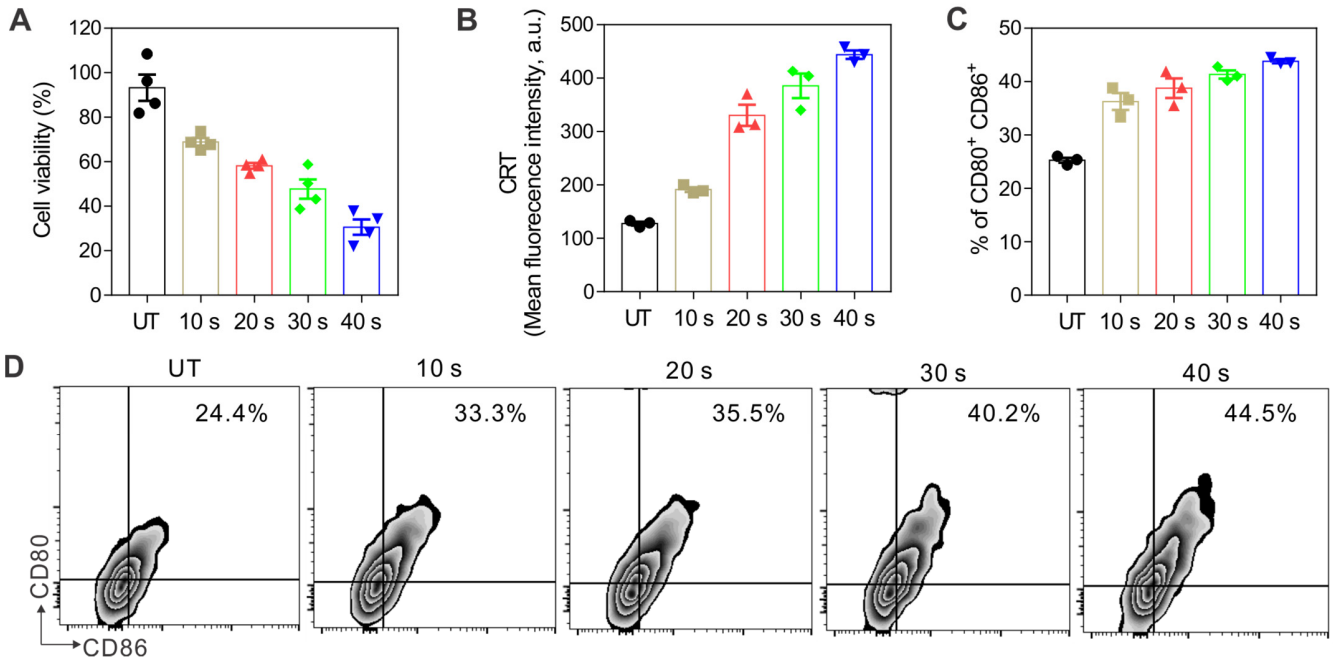

Fig. S4. (**A**) Cell viability of B16F10 melanoma cells after CAP treatment for different time (*n*=4). (**B**) Flow cytometry analyses showing the induction of the ICD marker CRT on B16F10 cells after CAP treatment (*n*=3). (**C**) *In vitro* activation of DCs ($CD86^+CD80^+$ cells) in response to CAP treatment for different time (*n*=3). (**D**) Representative flow cytometric analysis images of DC maturation induced by CAP treatment for different times. Data are presented as mean ± SEM.

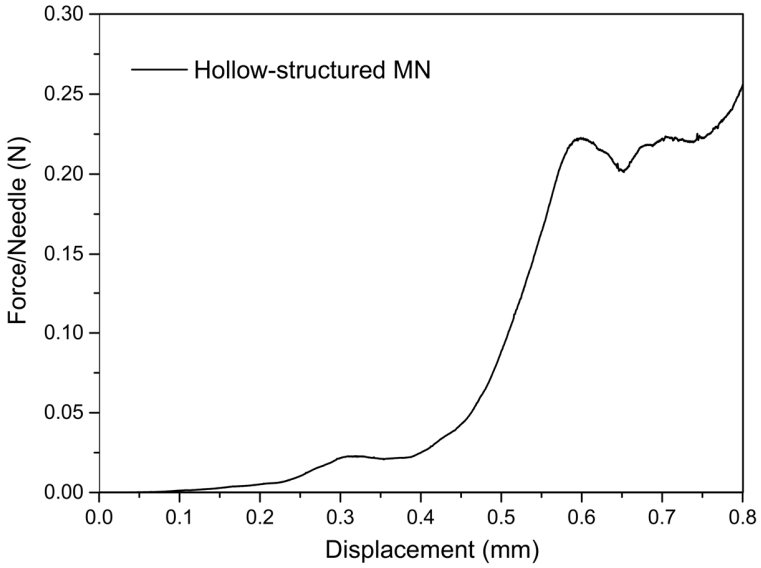

Fig. S5. Mechanical property of the hMN patch. The mean failure force is 0.23 N/needle.

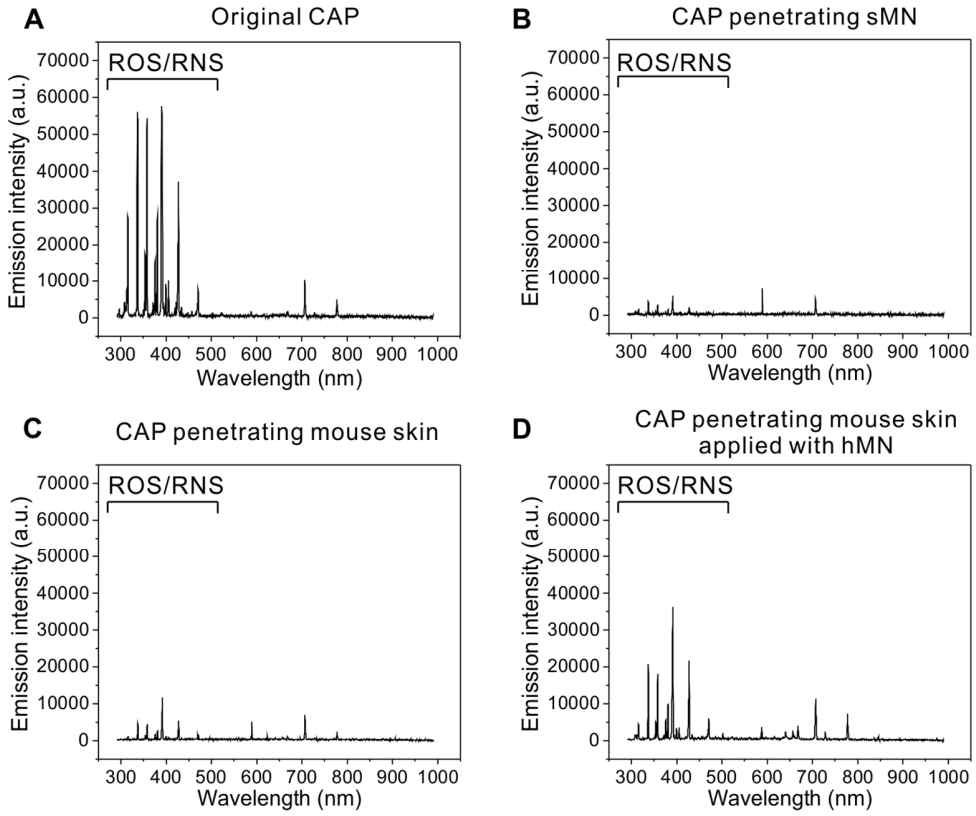

Fig. S6. The OES spectra of (**A**) original CAP, (**B**) CAP penetrating sMN, (**C**) CAP penetrating the mouse skin, and (**D**) CAP penetrating the mouse skin applied with hMN.

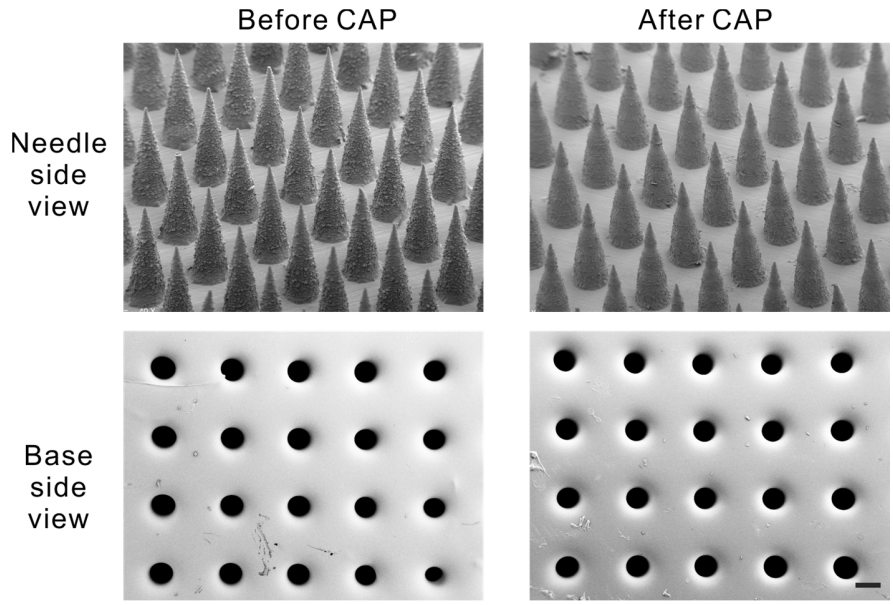

Fig. S7. Study of morphology changes of hMN patches after CAP treatment. No significant changes were observed. Scale bar: 200 μm.

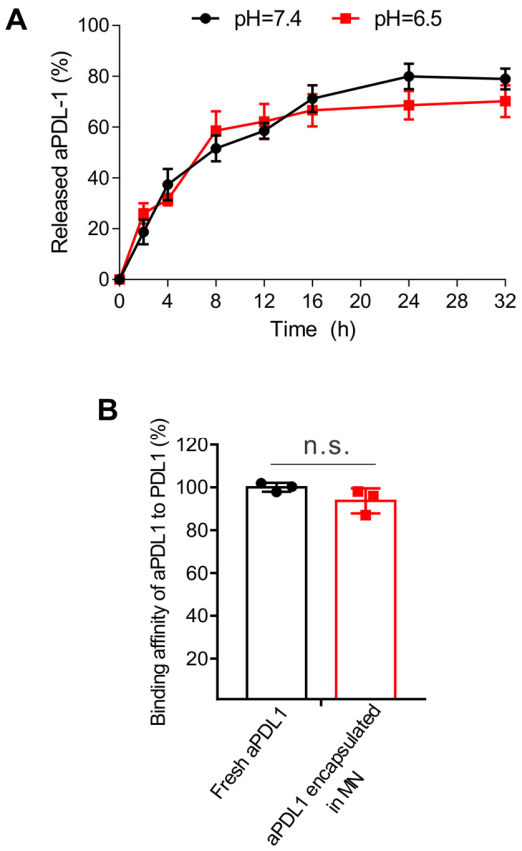

Fig. S8. (**A**) *In vitro* aPDL1 release profile from the hMN patch (*n*=3). (**B**) Binding affinity test of aPDL1 to PDL1 after encapsulation in MN. Data are presented as mean ± SEM (*n*=3). Data are presented as mean ± SEM. n.s., no significance.

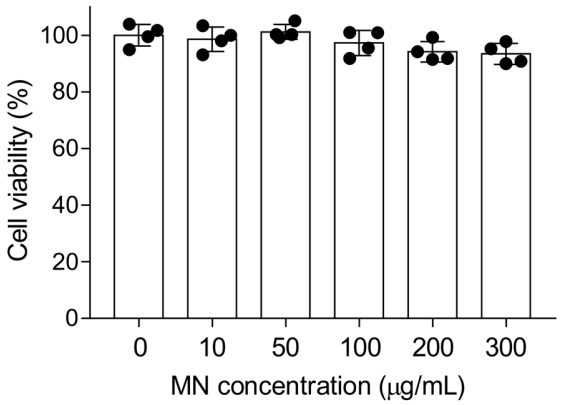

Fig. S9. Cytotoxicity study of the blank MNs. hMN patches were re-dissolved and added to B16F10 cells for 24 h of incubation. Data are presented as mean ± SEM (*n*=4).

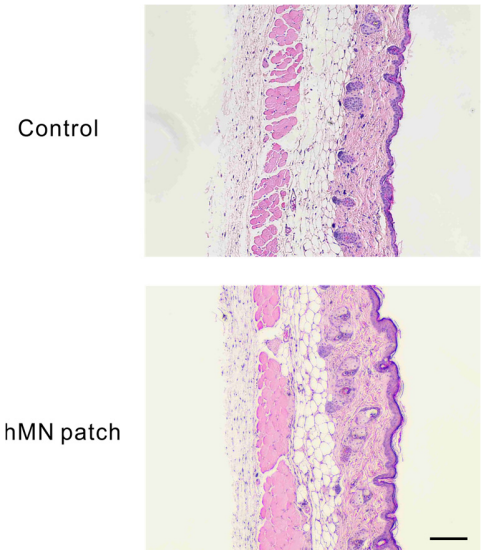

Fig. S10. H&E-stained skin sections collected from healthy mice or hMN-treated mice 3 days post-administration. Scale bar, 100 μm.

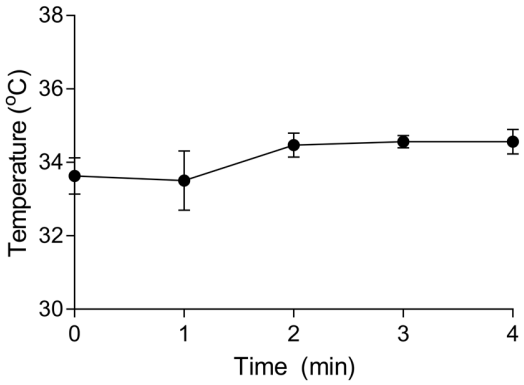

Fig. S11. Measurements of local temperature in the CAP-treated tumor area during CAP treatment in mice. Data are presented as mean ± SEM (n= 4).

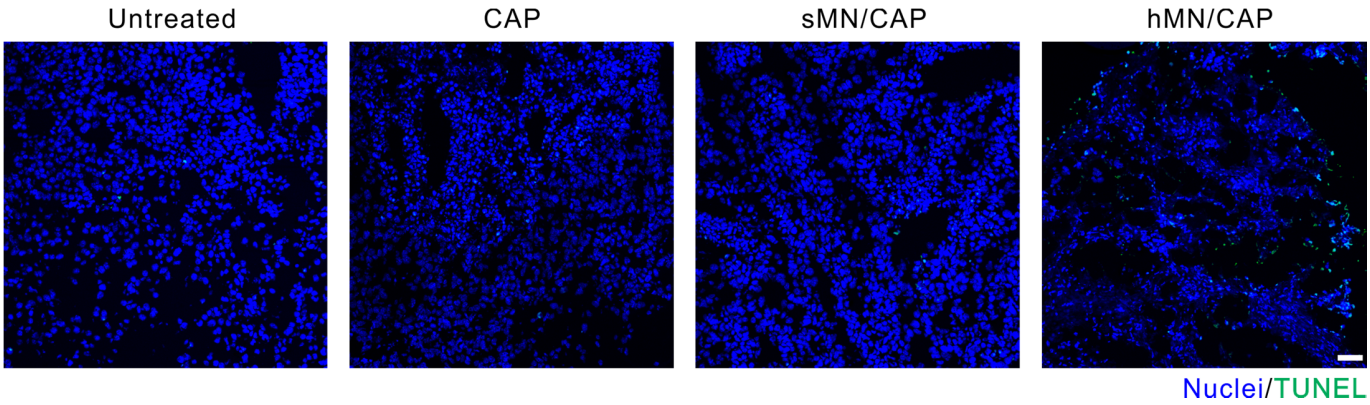

Fig. S12. TUNEL assays of tumor tissues three days after different treatments. Scale bar: 50 μm.

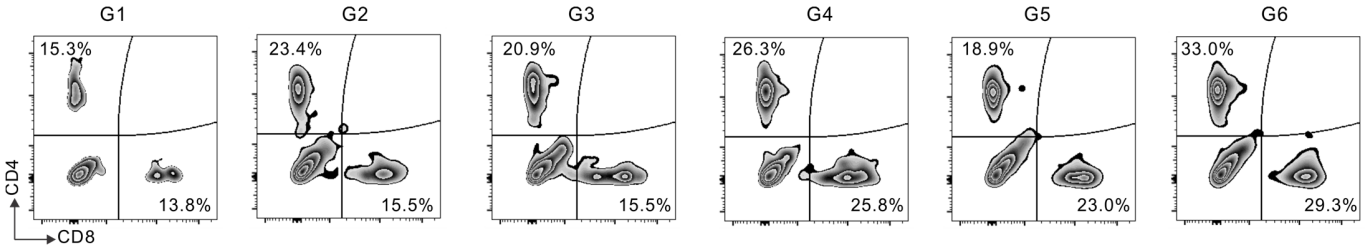

Fig. S13. Representative flow cytometric analysis of $CD4^+$ and $CD8^+$ T cells (gated on $CD3^+$ cells) in the tumors in different groups 3 days post-treatment (primary tumor model). G1, untreated; G2, CAP; G3, sMN/CAP; G4, hMN/CAP; G5, hMN-aPDL1; G6, hMN-aPDL1/CAP.

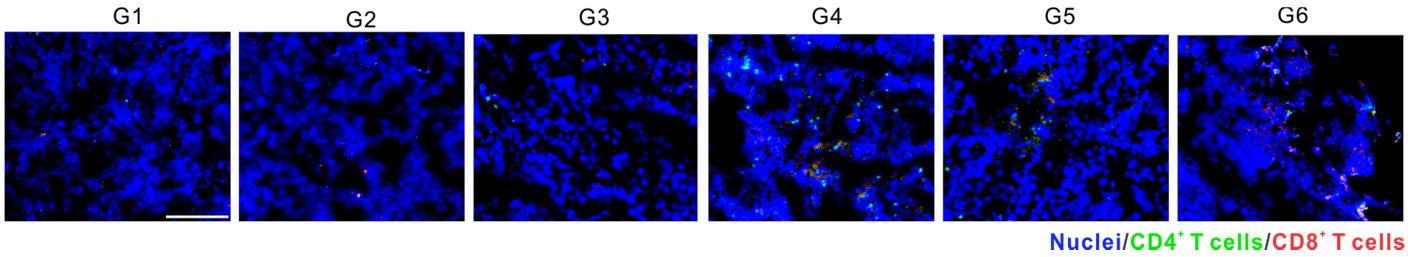

Fig. S14. Representative immunofluorescence staining of $CD4^+$ T cells and $CD8^+$ T cells in the tumors. G1, untreated; G2, CAP; G3, sMN/CAP; G4, hMN/CAP; G5, hMN-aPDL1; G6, hMN-aPDL1/CAP. Scale bar, 100 μm.

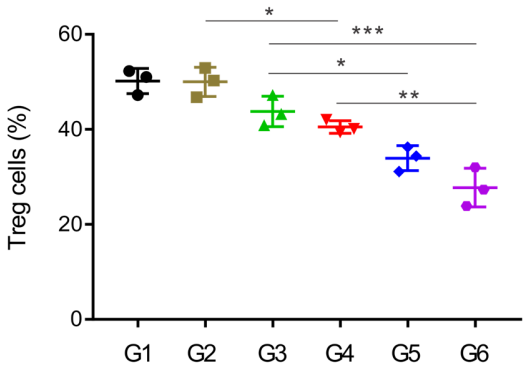

Fig. S15. Quantitative and representative flow cytometric analysis of Tregs cell within the tumors in different groups 3 days post-treatment (primary tumor model). Data are presented as mean ± SEM (n= 3). G1, untreated; G2, CAP; G3, sMN/CAP; G4, hMN/CAP; G5, hMN-aPDL1; G6, hMN-aPDL1/CAP. Statistical significance was calculated *via* one-way ANOVA with a Tukey post-hoc test. *P<0.05; **P<0.01; ***P< 0.001.

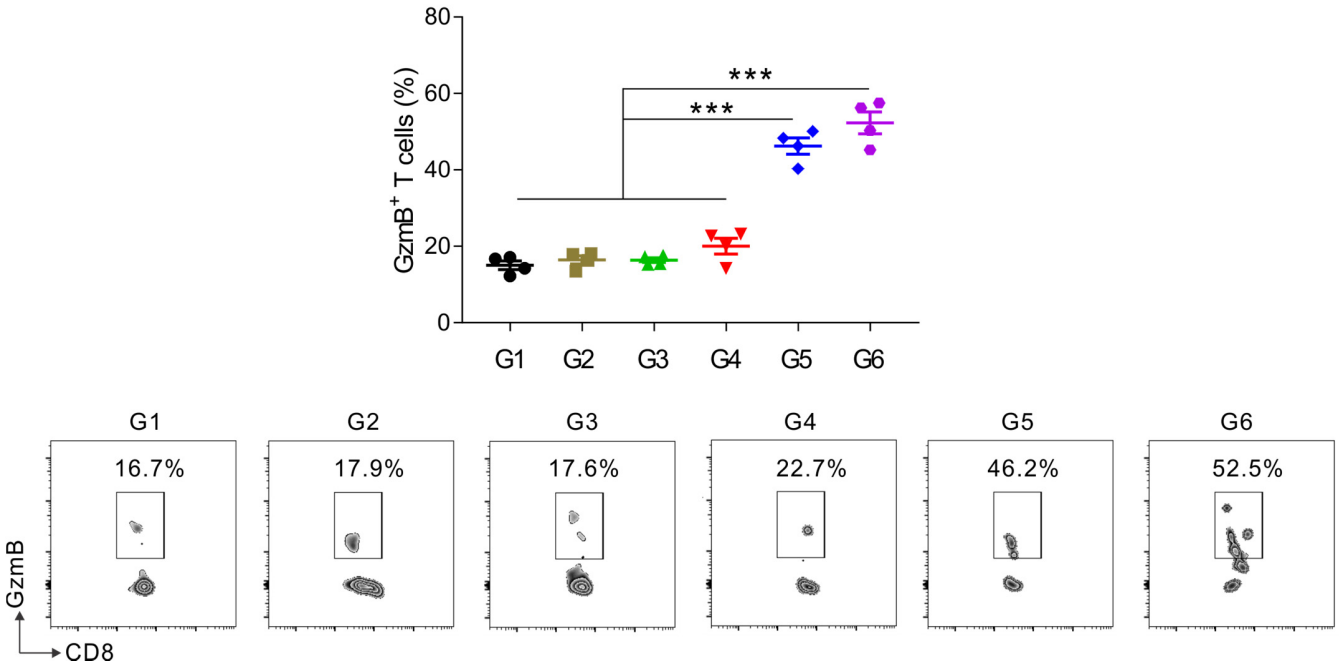

Fig. S16. Quantitative analysis and representative plots of GzmB in $CD8^+$ T cells within the tumors analyzed by the flow cytometry (gated on $CD8^+$ T cells) 3 days post-treatment (n=4). Data are presented as mean ± SEM. Statistical significance was calculated *via* one-way ANOVA with a Tukey post-hoc test for multiple comparisons. ***P< 0.001.

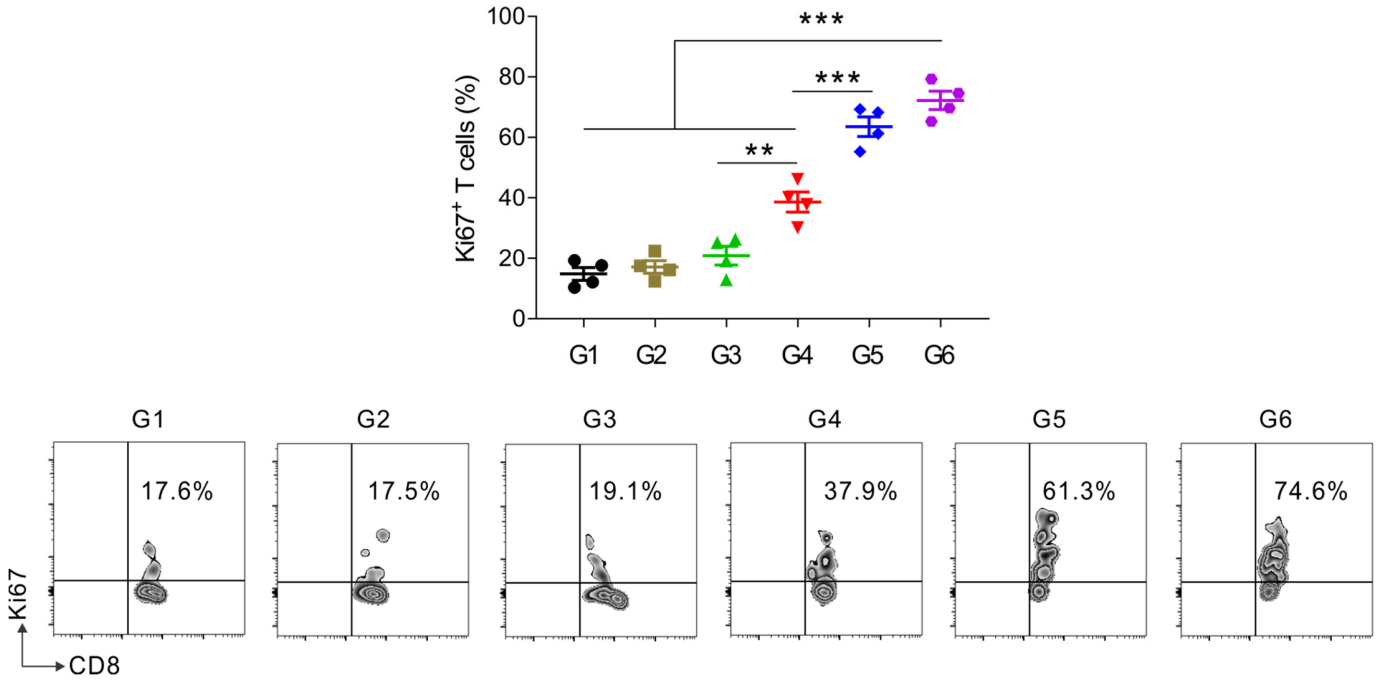

Fig. S17. Quantitative analysis and representative plots of Ki67 in $CD8^+$ T cells within the tumors analyzed by the flow cytometry (gated on $CD8^+$ T cells) 3 days post-treatment (n=4). Data are presented as mean ± SEM. Statistical significance was calculated *via* one-way ANOVA with a Tukey post-hoc test for multiple comparisons. $^{**}P< 0.01$; $^{***}P< 0.001$.

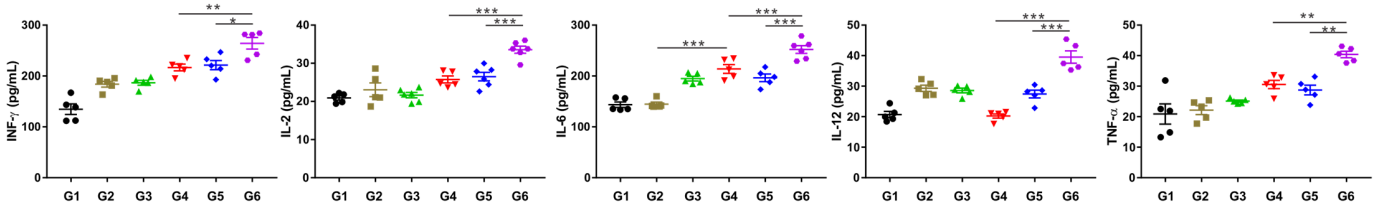

Fig. S18. Cytokine levels in the serum from mice isolated three days after different treatments (primary tumor model). Data are presented as mean ± SEM (n= 5). G1, untreated; G2, CAP; G3, sMN/CAP; G4, hMN/CAP; G5, hMN-aPDL1; G6, hMN-aPDL1/CAP. Statistical significance was calculated *via* one-way ANOVA with a Tukey post-hoc test. *P< 0.05; **P< 0.01; ***P< 0.001.

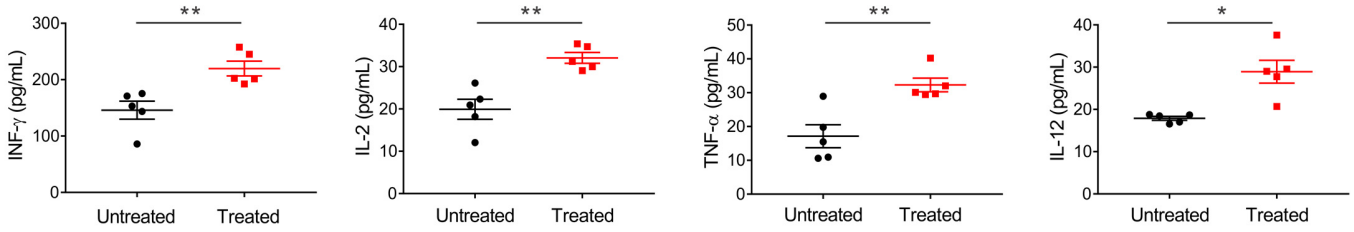

Fig. S19. Cytokine levels in the serum isolated three days after different treatments (distant tumor model). Data are presented as mean ± SEM (n = 5). Statistical significance was calculated *via* Student's *t*-test. *P < 0.05; **P < 0.01.

Movie S1 (separate file). A CLSM movie of a hollow-structured microneedle.

SI Reference

1. Q. Chen et al. (2016) Photothermal therapy with immune-adjuvant nanoparticles together with checkpoint blockade for effective cancer immunotherapy. *Nat Commun* **7**:13193.